The Thirty-First International Florida
Artificial Intelligence Research Society Conference (FLAIRS-31)

Spatiotemporal Associative Classification for Satellite Image Time Series

Carlos Roberto Silveira Junior, Marilde T. Prado Santos, Marcela Xavier Ribeiro
Department of Computing, Federal University of São Carlos
Washington Luís, km 235 – SP–310, 13565-905
São Carlos, São Paulo, Brazil

Abstract

Mining spatiotemporal data is a challenging task since time and space bring two complex variables to the mining analysis. Traditional classifiers consider the individual data instances alone disregarding the time and spatial correlations. This leads to a lessening of the analysis potential of the traditional mining to an analysis solely of a given time or space. In this paper, we propose a Spatiotemporal Associative Classifier, called SAC, able to catch time and spatial correlations in the classification task. To perform spatiotemporal classification SAC employs, as the learning model, Thematic Spatiotemporal Association Rules (TSAR). TSAR are association rules that track the relations of time and space and the evolution of the thematic attributes values. We employed SAC and TSAR to mine Satellite Image Time Series (SITS) in order to predict sun flares events. However, a TSAR has a difficult understanding, not treated previously in the literature. In this sense, this paper also employs the proposed classifier to improve its understanding by the domain specialist. The results presented high accuracies and are promising according to the domain specialists.

Introduction

The knowledge extraction from Satellite Image Time Series (SITS) is a challenging task. The SITS is a spatiotemporal and multidisciplinary data that includes image and text mining. Recently, the knowledge extraction from SITS has become more relevant due to the increase in its available data. Recent works have been proposed to extract patterns from this domain (Traore, Kamsu-Foguem, and Tangara 2017) and (Zhang et al. 2015), but the mined patterns still do not suit the domain-expert perspective. SITS are spatiotemporal data and most methods disregard time and spatial correlations. In order to support spatiotemporal mining of SITS, supporting the domain specialist, we proposed an Associative Classifier, called Spatiotemporal Associative Classifier (SAC). SAC has association rules as inputs and classifies the images features from SITS according to its spatiotemporal relations and frequency.

A TSAR is an association rule that shows an event evolution and its relation to other close events, often used for spatiotemporal data (Rao, Govardhan, and Rao 2012). However, a TSAR has a difficult understanding, not treated previously in the literature. In this sense, this paper also employs the proposed classifier to improve its understanding by the domain specialist.

That way, our hypotheses are: (a) the usage of TSAR as the learning model for an associative classifier makes the classifier able to treat spatiotemporal data, and; (b) the proposed classifier makes feasible the understanding of TSAR extracted from Solar SITS.

Our hypothesis is supported by the fact that Associative Classifiers are often used to make feasible data mining in domains composed of images, as the literature suggests. Moreover, it can be extended to spatiotemporal images domain as shown in this paper.

Background and Related Work

An associative classifier is a classifier whose learning model is a set of association rules (Atzmueller et al. 2015), (Thabtah 2007). Our proposal is an associative classifier based on votes that was introduced by (Ma and Liu 1998). An associative classifier based on votes counts how many times an item from the test instance occurs in the association rules set.

Formally, let a_i be an itemset from the database db; b_i be an item that represents a class label; and R be a set of association rules of the form $r_i : a_i \rightarrow b_i$ and $r_i \in R$. Given a new test instance $c = \{c_1, ...c_j, ...c_n\}$, an associative classifier, based on votes, counts how many times the items $a_i \in c_j$ was associated with b_i for all c_j in c and i in R. The class label b_i with the highest count value is given to the instance c as its label for the classifier.

Associative Classification based on votes is often used for image classification (Watanabe et al. 2010b). In that case, the idea is to associate the feature vector values extracted from images with the image classes. In (Watanabe et al. 2010b), (Watanabe et al. 2010a), and (Watanabe et al. 2012), associative classification based on vote are used in monographs domain. The authors had good results classifying tumors as benign or malignant or not-present.

(Alizadehsani et al. 2016) use an associative classifier to detect coronary artery disease. The authors proposed a model that is able to predict for each artery the chances of a coronary disease. The authors also claim that with this approach they have the best-predicted rate of the literature.

(Jiménez-Hernández et al. 2017) proposed an approach to creating classification models extensible for any domain - including images. The approach uses the concept of linear independence and probabilistic independence to create and optimize the models and the result is a framework able to classify new data. That work was not applied to spatiotemporal data; even though it is a generic approach.

The main difference between the previously presented works and our proposed approach is that they do not handle spatiotemporal data and do not consider the spatiotemporal correlations in the mining process. Our proposal increases the State of the Art since it is able to handle spatiotemporal data employing TSARs as the learning model of the associative classifier.

(Tucker et al. 2005) introduced a Bayesian classification method for visual characteristics with spatiotemporal relationships. To validate the proposal, a spatiotemporal ophthalmic database of glaucoma medical exams was used. Similarly, (Zahradnik and Skrbek 2013) propose two approaches for spatiotemporal data classification using neural networks: the first approach is based on MLP network and the second one is based on RBF network with two layers. Both works were not designed to handle the time variation in the classification task. That way, the labeled class represents the current data state and it cannot be used to predict the data behavior as we propose in this paper.

Spatiotemporal Associative Classifier

The Spatiotemporal Associative Classifier (SAC) is a Vote-based Associative Classifier developed to classify SITS images. First, the test image is submitted to a feature extractor, being represented by a feature vector. SAC returns the most likely label associated with the feature vector according to its learning model composed of TSARs (Thematic Spatiotemporal Association Rules).

The learning model of SAC is composed of r crisp TSARs of the form:

$$r : a \rightarrow b \ < \ sup,\ conf,\ time,\ space >$$

Where a and b are spatiotemporal itemsets not necessary disjointed; sup and $conf$ are the value of rule support and confidence; $time$ is the average period between the occurrence of a and the occurrence of b, and; $space$ is the average spatial distance between the items in a and the items in b.

Algorithm 1 presents the SAC algorithm. At Line 2, $Counter$ is set as empty. $Counter$ is hashmap data structure where the key is an image feature vector and the value is another hashmap, called sub-hashmap. The sub-hashmap key is a label that is associated with the feature vector and its value, and it is a quintuple: *counter, support, confidence, delta time and delta space*, which are information that comes from the association rules.

At Line 3, a loop is performed over each rule in the input set ($Rules$), where each rule is called r. At Line 4, $feature$ receives the feature vector in the antecedent of the rule r. If there is not any feature vector in the r antecedent then the loop is performed over the next rule.

At Line 5, $feature$ is checked to see if it is already in $Counter$. If it is, in Line 6 the algorithm calls $update$ to the sub-hashmap (also called node) of $feature$. Otherwise, in Line 8, a sub-hashmap is created and initialized as empty and $update$ is called over this new sub-hashmap. At the end of this loop, all rules are processed, and $Counter$ has required information about the $Rules$.

At Line 11, the output Map is initialized as empty. At Line 12, the rule iterates over the $Counter$ getting each sub-hashmap (node), called n.

At Line 13, c is created getting the most voted label. I.e. c gets the tuple that has the highest $count$ value (see the Algorithm 2 explanation). his operation is performed by $mostVoted$ function. From Line 14 to 17, the values of *support, confidence, delta space and delta time* are updated. The averages of those values are also calculated (by $update$ function). At Line 18, c is added to the output Map.

Data: $Rules$: Set of TSARs (Thematic Spatiotemporal Association Rules)
Result: Map : Feature values and their class labels

```
1  begin
2      Counter ← ∅ ;
3      for rule r ∈ Rules do
4          feature ← featureIn(r.antecendent) ;
5          if feature ∈ Counter then
6              update(Counter.get(feature), r) ;
7          else
8              update(Counter.new(feature), r) ;
9          end
10     end
11     Map ← ∅ ;
12     for node n ∈ Counter do
13         c ← mostVoted(n) ;
14         c.sup ← c.sup / c.count ;
15         c.conf ← c.conf / c.count ;
16         c.time ← c.time / c.count ;
17         c.space ← c.space / c.count ;
18         Map ← Map ⋃ c ;
19     end
20 end
```

Algorithm 1: The Spatiotemporal Associative Classifier (SAC).

Algorithm 2 presented the $update$ function. It takes the $node$ (sub-hashmap) that will be updated and the rule, $rule$ that is updating the $node$.

At Line 2, it makes a loop over $rule$'s consequence getting all labels, called l during the loop. A label is a non-feature vector item. If there rule has non label in its consequence, $update$ function does update $node$. Otherwise, Line 3, it will check if l is already part of $node$. If it is, Line 4, sn receives a reference for the quintuple (sub-hashmap value). If it is not, Line 6, a quintuple is created and initialized with zero in each value and it is associated with the l. At Line 8, the vote is updated, adding one to $sn.count$. From Line 9 until 12, the values of support, confidence, delta time and delta space is accumulated to sn. Those values came directly from the thematic spatiotemporal association rule called $rule$. At

Line 13, $node$ is updated.

Data: $node$: Map node to be updated. $rule$: rules.

1 **begin**
2   **for** $label\ l \in rule.consequence$ **do**
3   **if** $l \in node$ **then**
4             $sn \leftarrow node.getSubnode(l)$;
5   **else**
6             $sn \leftarrow newSubnode(node, l)$;
7   **end**
8         $sn.count \leftarrow sn.count + 1$;
9         $sn.sup \leftarrow sn.sup + rule.sup$;
10         $sn.conf \leftarrow sn.conf + rule.conf$;
11         $sn.time \leftarrow sn.time + rule.time$;
12         $sn.space \leftarrow sn.space + rule.space$;
13         $node \leftarrow node \bigcup sn$;
14   **end**
15 **end**

Algorithm 2: Update Function for the Map node.

The $mostVoted$-function, in Algorithm 1 find the most voted (highest $count$) associated with the image feature vectors. This step is also called ***SAC Low- Level Image Classification*** because it produces rules that show the most common associations for the training images according to their feature vectors.

Consider as an example of the set $Rules$ in Algorithm 1 the set: $\{r_1 : v_a \rightarrow l_a, r_2 : v_b \rightarrow v_c\ l_a, r_3 : v_a\ v_b\ l_a \rightarrow l_b\}$. Where r_i are rules, v_j are feature vectors and l_k are labels.

For r_1, $feature$ receives v_a that is not in $Counter$ (since it is the first iteration, it is empty). A new sub-hashmap is created in the $update$-function and l_a is added to that. Its $count$ starts with one. The support, confidence, delta time, and delta space are updated with r_1 values.

The same processing happens to r_2. However, r_2 has v_c in its consequent, $Counter(v_b)$ will not have v_c since it is not a label. The processing of r_3 updates v_a and v_b, adding one to l_b in each $v_{a,b}$. As the result, since $v_{a,b}$ has the same votes for $l_{a,b}$, Map has the association $v_a : l_a$, $v_a : l_b$, $v_b : l_a$, and $v_b : l_b$.

At last step, a test image feature vector is submitted to the ***SAC Low- Level Image Classification*** rules and the consequent of the rules satisfied by the test image are employed to label it.

Experiments, Results, and Discussion

In this section, we present three sets of experiments, for each database pre-proceed with different feature extractors: Histogram, Haralick (Haralick, Shanmugam, and Dinstein 1973), and SURF (Bay, Tuytelaars, and Van Gool 2006).

We employed a set of TSARs previously extracted employing Minimum support of 1%; Minimum confidence of 75% and maximum of spatial distance of 150 by $10,000$ parts of the solar disk, and; maximum of time variance of 20 days.

The input TSARs have the format $a \rightarrow b$, where a-itemset occurs before b-itemset.

The database is composed of 10300 sunspots records split by day, in the period from August 25, 2007, to August 24, 2016. It is represented by 70000 processed feature vectors.

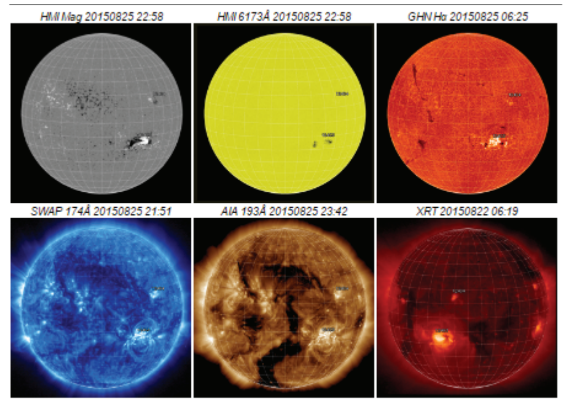

Figure 1: Example of one-day images of NOAA Satellite.

Today's/Yesterday's NOAA Active Regions

NOAA Number	Latest Position	Hale Class	McIntosh Class	Sunspot Area [millionths]	Number of Spots	Recent Flares
12403	S15W32 (487",-340")	βγδ/βγδ	Fkc/Ekc	0930/0760	47/66	C2.2(19:23) C1.3(18:01) C1.1(14:48) C1.3(12:33) C2.3(11:55) C2.3(07:58) C4.3(06:18) C1.1(04:14) / -
12404	N14W45 (653",148")	β/β	Cro/Cro	0020/0030	04/07	-

Figure 2: Example of Textual Data for the images.

Figure 1 and Figure 2 present an example of one-day data from NOAA Satellite. For each day, 6 images from the Solar Disk are taken with 6 different wavelengths. In addition, the Solar Disk can present several sunspots. The data (feature vector and textual data) of each sunspot are the input data for the TSARs mining and the SAC method.

The NOAA Satellite data are also composed of textual data that describes each sunspot, as presented by Figure 2. In the textual data, the sunspot is classified by its radioactive intensity (Hale Class) and by its morphology (McIntosh Class). Due to Hale is a subclass that can be extracted from McIntosh, we only employed the McIntosh Class.

The three experiments were performed over the same data however with different types of feature vectors, on a machine with 8 GB of RAM memory, 500 GB of HD and processor Intel Due Core 2.53 GHz. Java version 8 was used to implement the method. The operational system was an Arch Linux 64 bits.

Figure 3, 6 and 7 present the low-level classifications of solar image features generated by SAC using respectively the following low-level features: histogram, Haralick texture and SURF shape.

In Figure 3, the $C1$-classification rule presents an association of the visual characteristic $(3627361.000; 3632207.000)$, $(3113326.000; 3119009.000)$ with Cao-McIntosh. The support average of the rules having this association is 19.4% and the confidence average of these rules is 78.9%. These rules present a variation in the average time of 5.067 days between the antecedent (cause) and consequent. In addition, there is a variation in the distance between the sunspots that

```
C1:
(3627361.000;3632207.000],(3113326.000;
3119009.000], 0010 : Cao
sup=0.194 conf=0.789 time=5.067 space=62.813

C2:
(3853748.000;3856799.000],(2894258.000;
2897071.000], 0010 : Axx
sup=0.019 conf=0.83 time=3.781 space=72.814

C3:
(3590618.000;3597197.000],(3150223.000;
3154539.000], 0060 : Cro
sup=0.023 conf=0.778 time=6.64 space=3.598
```

Figure 3: Result of the SAC low-level classification of visual features using histogram.

are associated with 62,813 on the mean. Figure 4 presents an image being classified by the of $C1$-classification rule. The 12201-sunspot at November 3rd, 2014 has the visual feature of $C1$ antecedent and two other sunspots close to an average of 62.813 parts of the solar disk, 12200-sunspot, and 12204-sunspot. The $C1$ rule says that in at the average of 5 days the sun image will have two close sunspots of Cao-McIntosh with the Cao-McIntosh classification, what really occurred in the image of November 6th, 2014.

The $C2$-classification rule presents an association of the visual characteristic $(3853748.000; 3856799.000)$, $(2894258.000; 2897071.000)$ of a sunspot whose size is 10 parts of the solar disk with Axx-McIntosh. The rules support average that contributed to this association is 1.9% and the trust is 83%. The average of time occurrence is 3,781 days and the average of space is 72.814 parts of the solar disk. Figure 5 presents an example of $C2$-classification. The 12643-sunspot at March 26th, 2017 has the visual characteristic of $C2$ and another sunspot close to an average of 72.814 parts of the solar disk, 12644-sunspot. The rule $C2$ says that in 3.7 days a sunspot of Axx-McIntosh class should occur. That really occurs on March 29th, 2017, when the 12643-sunspot presents the classification Axx-McIntosh; also, the 12644-sunspot is still close to 12643-sunspot.

The $C3$-classification rule presents an association of the visual characteristic $(3590618.000; 3597197.000)$, $(3150223.000; 3154539.000)$ of a sunspot whose size is 60 parts of the solar disk with Cro-McIntosh. The average support of the rules that contributed to this association is 2.3% and the trust is 77.8%. The mean time is 6.64 days and space is 3,598 parts of the solar disk on average.

In Figure 6, the $C4$-classification rule presents an association of the visual characteristic $(-0.350; 0.341), (9.764; 23.692)$, $(30339.404; 31432.453), (4949.939; 4952.800)$ $ldots$ of a sunspot whose size is 30 parts of the solar disk with Dso -McIntosh. The average support of the rules that contributed to this association is 18.2% and the confidence average is 76.7%. The time is 2,609 days and space is of 44,885 parts of the solar disk on average.

The $C5$-classification presents an association of the visual characteristic $(-0.350; 0.341], (9.764; 23.692)$, $(45521.675; 45809.851), (7083.643; 7088.084)$ $ldots$ of a sunspot whose size is 110 parts of the solar disk with Axx-McIntosh. The average support of the rules that contributed to this association is 2.2% and the confidence average is 93.8%. The time is 2,583 days and space is 69,508 parts of the solar disk on average.

The $C6$-classification presents an association of the visual characteristic $(-0.350; 0.341), (9.764; 23.692)$, $(29061.805; 30339.404), (4964.073; 4967.090)$ $ldots$ of a sunspot whose size is 300 parts of the solar disk with Dso-McIntosh. The average support of the rules that contributed to this association is 17.8% and the confidence average is 81%. The time is 2,477 days and space is 73,351 parts of the solar disk on average.

In Figure 7, the $C7$-classification presents an association of the visual characteristic $(784, 896; 785, 216), (14, 534; 15, 198)\ldots$ of a sunspot whose size is 20 parts of the solar disk with Axx-McIntosh is presented. The average support of the rules that contributed to this association is 22.7% and the trust is 100%. The average variation in time is 1 days and there is no variation in space, this indicates an evolution of the spot itself without the need to be associated with another spot for this behavior.

The $C8$-classification presents an association of the visual characteristic $(776, 995; 777, 279), (14, 534; 15, 198)\ldots$ of a sunspot whose size is 10 parts of the solar disk with Dro-McIntosh. The average support of the rules that contributed to this association is 6.3% and the trust is 100%. The average variation in time is 2 days and the variation in space is 23,005 parts of the solar disk on average.

The $C9$-classification presents a visual characteristic association is shown $(664, 769; 665, 061), (14, 534; 15, 198)\ldots$ of a sunspot whose size is 30 parts of the solar disk with Axx-McIntosh. The average support of the rules that contributed to this association is 5.3% and the trust is 100%. The average variation in time is 5.536 days and the variation in space is 42.423 parts of the solar disk on average.

To verify the results, we used a small database of images containing the March 2017 images -138 images with an average of 3 sunspots each day. The precision variates according to the feature extract used: For histogram 82.7% of precision, for Haralick 84.1%, for SURF 87.3%. This is a good preliminary result for SAC; however, more experiments must be performed to validate SAC.

Conclusion and Future Works

Associative classification is an approach to build a classification system from association rules. In this paper, we proposed an Associative Classifier based on votes for SITS, called Spatiotemporal Associative Classifier (SAC). SAC differs from the state of the art works because it can track spatial and temporal evolution in the learning model, by using Thematic Spatiotemporal Association Rules (TSAR). TSAR are association rules that consider the relationship between close events and their evolving. SAC constructs a

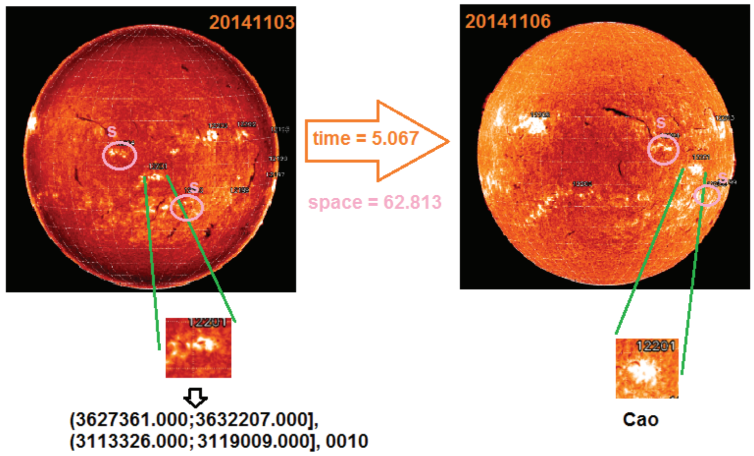

Figure 4: Example of the classification of the left image using the $C1$ classification rule.The $C1$ rule says that in at the average of 5 days the sun image will have two close sunspots of Cao-McIntosh with the Cao-McIntosh classification, what really occurred on the right image.

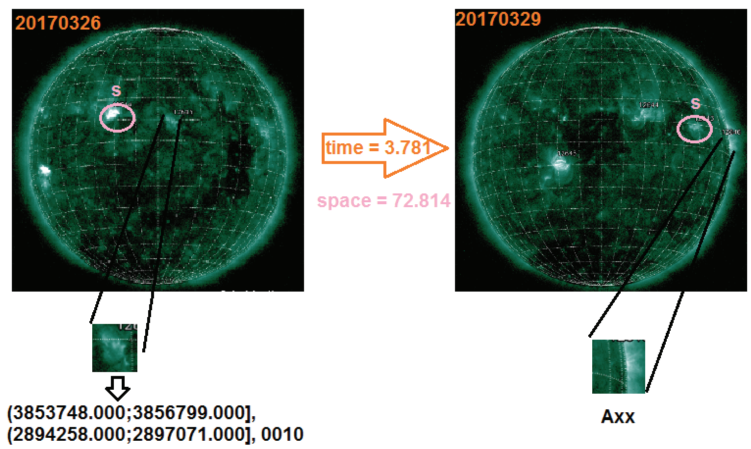

Figure 5: Example of the classification of the left image using the $C2$ classification rule. The rule $C1$ says that in 3,7 days a sunspot of Axx-McIntosh class should occur, what really occurred on the right image.

learning model to perform a low-level feature vector classification based on time and space co-occurrences of the events. The results indicate that SAC can be used to predict the solar behavior with high accuracy.

As future work, we will use a bigger database to validate the classifier and a visualization interface will be implemented allowing a better analysis of the data and the extracted patterns. It is also part of future works add support for distributed processing aims to brings better performance and support to fuzzy image feature vectors.

Acknowledgment. The authors thank the SolarMonitor. org for free providing of the solar data; the *Instituto Nacional de Pesquisas Espaciais* (INPE); and, the Astrophysics Researcher José Roberto Cecatto for the support in data understanding and analysis. We also thank CAPES, CNPq and FAPESP.

References

Alizadehsani, R.; Zangooei, M. H.; Hosseini, M. J.; Habibi, J.; Khosravi, A.; Roshanzamir, M.; Khozeimeh, F.; Sarrafzadegan, N.; and Nahavandi, S. 2016. Coronary artery disease detection using computational intelligence methods. *Knowledge-Based Systems* 109:187 – 197.

Atzmueller, M.; Kibanov, M.; Hayat, N.; Trojahn, M.; and Kroll, D. 2015. Adaptive class association rule mining for human activity recognition. In *MUSE@ PKDD/ECML*, 19–34.

Bay, H.; Tuytelaars, T.; and Van Gool, L. 2006. Surf: Speeded up robust features. In *European conference on computer vision*, 404–417. Springer.

Haralick, R. M.; Shanmugam, K.; and Dinstein, I. 1973. Textural features for image classification. *IEEE Transactions on Systems, Man, and Cybernetics* SMC-3(6):610–621.

```
C4:
(-0.350;0.341],(9.764;23.692],(30339.404;
31432.453],(4949.939;4952.800],(0.341;4.240],
(9.764;23.692],(508.144;519.027],... 0030 : Dso
sup=0.182 conf=0.767 time=2.609 space=44.885

C5:
(-0.350;0.341],(9.764;23.692],(45521.675;
45809.851],(7083.643;7088.084],(0.341;4.240],
(24.262;28.389],(461.257;461.907],... 0110 : Axx
sup=0.022 conf=0.938 time=2.583 space=69.508

C6:
(-0.350;0.341],(9.764;23.692],(29061.805;
30339.404],(4964.073;4967.090],(0.341;4.240],
(9.764;23.692],(519.027;657.910],...  0300 : Dso
sup=0.178 conf=0.81 time=2.477 space=73.351
```

Figure 6: Result of the SAC low-level classification of visual features using Haralick.

```
C7:
(784.896;785.216],(14.534;15.198],... 0020 : Axx
sup=0.227 conf=1 time=1 space=0

C8:
(776.995;777.279],(14.534;15.198],... 0010 : Dro
sup=0.063 conf=1 time=2 space=23.005

C9:
(664.769;665.061],(14.534;15.198],... 0030 : Axx
sup=0.053 conf=1 time=5.536 space=42.423
```

Figure 7: Result of the SAC low-level classification of visual features using SURF.

Jiménez-Hernández, H.; Herrera-Navarro, A.-M.; Barriga-Rodríguez, L.; Córdova-Esparza, D.-M.; and González-Barbosa, J.-J. 2017. A framework for developing associative classifiers based on ica. *Engineering Applications of Artificial Intelligence* 58:88–100.

Ma, B. L. W. H. Y., and Liu, B. 1998. Integrating classification and association rule mining. In *Proceedings of the fourth international conference on knowledge discovery and data mining*.

Rao, K. V.; Govardhan, A.; and Rao, K. C. 2012. Spatiotemporal data mining: Issues, tasks and applications. *International Journal of Computer Science & Engineering Survey (IJCSES) Vol* 3:39–52.

Thabtah, F. 2007. A review of associative classification mining. *The Knowledge Engineering Review* 22(1):37–65.

Traore, B. B.; Kamsu-Foguem, B.; and Tangara, F. 2017. Data mining techniques on satellite images for discovery of risk areas. *Expert Systems with Applications* 72:443 – 456.

Tucker, A.; Vinciotti, V.; Liu, X.; and Garway-Heath, D. 2005. A spatio-temporal bayesian network classifier for understanding visual field deterioration. *Artificial Intelligence in Medicine* 34(2):163 – 177.

Watanabe, C. Y.; Ribeiro, M. X.; Traina Jr, C.; and Traina, A. J. 2010a. Sacminer: A new classification method based on statistical association rules to mine medical images. In *ICEIS*, 249–263. Springer.

Watanabe, C. Y.; Ribeiro, M. X.; Traina Jr, C.; and Traina, A. J. 2010b. Statistical associative classification of mammograms-the sacminer method. In *ICEIS*, 121–128.

Watanabe, C. Y. V.; Ribeiro, M. X.; Traina, A. J. M.; and Jr, C. T. 2012. A statistical associative classifier with automatic estimation of parameters on computer aided diagnosis. In *2012 11th International Conference on Machine Learning and Applications*, volume 1, 564–567.

Zahradnik, J., and Skrbek, M. 2013. Spatio-temporal data classification using cvnns. *Simulation Modelling Practice and Theory* 33(Supplement C):81 – 88. EUROSIM 2010.

Zhang, S.; Zheng, X.; Wang, Q.; Fan, Y.; Ma, X.; and Hao, X. 2015. New satellite image associative classification algorithm based on gabor texture. *Remote Sensing and Smart City* 64:257.